

A kinetic study of analyte–receptor binding and dissociation for biosensor applications: a fractal analysis for two different DNA systems

Anand Ramakrishnan, Ajit Sadana*

Chemical Engineering Department, University of Mississippi, 134 Anderson Hall, University, MS 38677-9740, USA

Received 31 October 2001; received in revised form 1 July 2002; accepted 1 July 2002

Abstract

A fractal analysis of DNA binding and dissociation kinetics on biosensor surfaces is presented. The fractal approach provides an attractive, convenient method to model the kinetic data taking into account the effects of surface heterogeneity brought about by ligand immobilization. The fractal technique can be used in conjunction or as an alternate approach to conventional modeling techniques, such as the Langmuir model, saturation model, etc. Examples analyzed include a DNA molecular beacon biosensor and a plasmid DNA–(cationic polymer) interaction biosensor. The molecular beacon example provides some insights into the nature of the surface and how it influences the binding rate coefficients. The DNA–cationic polymer interaction example provides some quantitative results on the binding and dissociation rate coefficients. Data taken from the literature may be modeled, in the case of binding, using a single-fractal analysis or a dual-fractal analysis. The dual-fractal analysis results indicate a change in the binding mechanism as the reaction progresses on the surface. A single-fractal analysis is adequate to model the dissociation kinetics in the example presented. Relationships are presented for the binding rate coefficients as a function of their corresponding fractal dimension, D_f , which is an indication of the degree of heterogeneity that exists on the surface. When analyte–receptor binding is involved, an increase in the heterogeneity of the surface (increase in D_f) leads to an increase in the binding rate coefficient.

© 2002 Elsevier Science Ireland Ltd. All rights reserved.

Keywords: DNA biosensors; Binding and dissociation rate coefficients; Fractal dimensions; Heterogeneity

1. Introduction

Biosensor technology is an exciting and promising development in bioanalytical research. These

sensors or biosensors may be utilized to monitor the analyte–receptor reactions in real time (Myszka et al., 1997). In addition, some techniques such as the surface plasmon resonance (SPR) biosensor, do not require radiolabeling or biochemical tagging (Jonsson et al., 1992), are reusable, have a flexible experimental design, provide a rapid and automated analysis, and have a

* Corresponding author. Tel.: +1-662-915-5349; fax: +1-662-915-7023

E-mail address: cmsadana@olemiss.edu (A. Sadana).

completely integrated system. Also, the SPR in combination with mass spectrometry (MS) exhibits the potential to provide a proteomic analysis (Williams and Addona, 2000). With so many distinct advantages it is not surprising that biosensors are finding increasing usage and applications in the fields of biotechnology, physics, chemistry, genomics, medicine, cell-monitoring systems, aviation, oceanography, and environmental control.

There is a need to characterize the reactions occurring at the biosensor surface in the presence of diffusional limitations that are inevitably present in these types of systems. It is essential to characterize not only the associative or binding reaction (by a binding rate coefficient, k_{bind} or k_{ads}), but also the desorption or dissociation reaction (by a desorption rate coefficient, k_{des} or k_{diss}). This information assists significantly in enhancing the biosensor performance parameters, such as reusability, multiple usage for the same analyte, and stability, besides providing further insights into sensitivity, reproducibility, and specificity of the biosensor. The ratio of k_{diss} to k_{bind} (equal to K_D) may be used to help further characterize the biosensor–analyte–receptor system. The analysis to be presented here is, in general, applicable to ligand–receptor and analyte–receptorless systems for biosensor and other applications (e.g. membrane–surface reactions).

Kopelman (1988) indicates that surface diffusion-controlled reactions that occur on clusters or islands are expected to exhibit anomalous and fractal-like kinetics. These fractal kinetics exhibit anomalous reaction orders and time-dependent coefficients (e.g. binding or dissociation). Fractals are disordered systems with the disorder described by nonintegral dimensions (Pfeifer and Obert, 1989). Kopelman (1988) further indicates that as long as surface irregularities show scale invariance that has dilatational symmetry, they can be characterized by a single number, the fractal dimension. The fractal dimension is a global property and is insensitive to structural or morphological details (Pajkossy and Nyikos, 1989). Markel et al. (1991) indicate that fractals are scalable, self-similar mathematical objects that possess non-trivial geometrical properties.

Furthermore, these investigators indicate that rough surfaces, disordered layers on surfaces, and porous objects all possess fractal structure.

A biosensor surface along with the immobilized ligand is a good example of a disordered system or a rough surface. The biosensor surface we study here may also reasonably fall into this class of surfaces. The roughness of the biosensor surface is due mainly to the nature of the sensor chip surface or the nature of the immobilized ligand. It may also stem from the immobilization method or the chemistry. Though we do not present any physical evidence or independent proof regarding the heterogeneous nature of the biosensor surface, given the above factors, it is not an unreasonable assumption to make.

A consequence of the fractal nature of these systems is a power-law dependence of a correlation function (in our case analyte–receptor complex on the surface) on a coordinate (e.g. time). This fractal nature or power-law dependence is exhibited during both the association (or binding) and/or the dissociation phases. In other words, the degree of roughness or heterogeneity on the surface affects both the association or binding of the analyte to the receptor on the surface, and also the dissociation of the analyte–receptor complex on the surface. However, the influence of the degree of heterogeneity on the surface may affect these two phases differently. Also, since this is a temporal reaction, and presumably the degree of heterogeneity may be changing with (reaction) time, there may be two (or more) different values of the degree of heterogeneity for the association and the dissociation phases.

Fractal aggregate scaling relationships have been determined for both diffusion-limited and diffusion-limited scaling aggregation processes in spatial dimension 2, 3, 4, and 5 (Sorenson and Roberts, 1997). Basically, this means that the fractal approach is applied to binding reactions in the presence of diffusional limitations, in which case the kinetics is affected both by the heterogeneity as well as mass-transfer limitations and as the reaction progresses over time, the fractal nature is lost and only regular diffusion is now present.

This is one possible justification for analyzing the diffusion-limited binding and dissociation kinetics assumed to be present in all of the systems analyzed. The parameters thus obtained would provide a useful comparison of different situations. Alternate expressions involving saturation, first-order reaction, and no diffusion limitations are possible, but they are deficient in describing the heterogeneity that exists inherently on the surface.

We will obtain values of the fractal dimensions and the rate coefficient values for the association (binding) as well as the dissociation phase, for (i) binding of oligonucleotide in solution to biotinylated immobilized ssDNA molecular beacon on a SPR biosensor (Liu et al., 2000), and (ii) binding of plasmid DNA in solution to thiolated and non-thiolated poly(L-lysine) immobilized on a SPR biosensor surface (Wink et al., 1999). The analysis should assist significantly in enhancing the relevant biosensor performance parameters. It must be understood that it might not always be possible to control the surface heterogeneity, but a fractal analysis gives us an indication regarding the nature of the surface. This might be helpful for experimentalists as they can think of improving biosensor performance characteristics by either changing the type of biosensor chip, the ligand molecule (for e.g. monoclonal antibodies) or by exerting a greater control over the immobilization conditions.

2. Theory

Havlin (1989) has reviewed and analyzed the diffusion of reactants towards fractal surfaces. The details of the theory and the equations involved for the binding and the dissociation phases for analyte–receptor binding are available (Sadana, 2001). The details are not repeated here; except that just the equations are given to permit easier reading. The equations have been applied to other biosensor systems (Sadana, 2001; Ramakrishnan and Sadana, 2001). Here we will attempt to apply these equations to (a) the binding of a non-complementary oligonucleotide and 1-base mismatch oligonucleotide for a hybridization reaction

using an immobilized beacon optical fiber biosensor (Liu et al., 2000), and (b) the interaction between plasmid DNA and cationic polymers (Wink et al., 1999).

2.1. Single-fractal analysis

2.1.1. Binding rate coefficient

Havlin (1989) indicates that the diffusion of a particle (analyte) from a homogeneous solution to a solid surface (e.g. receptor-coated surface) on which it reacts to form a product (analyte–receptor complex) is given by:

$$(\text{analyte.receptor}) \sim \begin{cases} t^{(3-D_{f,\text{bind}})/2} = t^p (t < t_c) \\ t^{1/2} (t > t_c) \end{cases} \quad (1a)$$

Here $D_{f,\text{bind}}$ or D_f (used later in the manuscript) is the fractal dimension of the surface during the binding step. t_c is the crossover value. Eq. (1a) indicates that the concentration of the product $\text{Ab.Ag}(t)$ in a reaction $\text{Ab} + \text{Ag} \rightarrow \text{Ab.Ag}$ on a solid fractal surface scales at short and intermediate time scales as $[\text{Ab.Ag}] \sim t^p$ with the coefficient $p = (3 - D_{f,\text{bind}})/2$ at short time scales, and $p = 1/2$ at intermediate time scales.

Havlin (1989) indicates that the crossover value may be determined by $r_c^2 \sim t_c$. Above the characteristic length, r_c , the self-similarity is lost. Above t_c , the surface may be considered homogeneous, since the self-similarity property disappears, and “regular” diffusion is now present. For the present analysis, t_c is chosen arbitrarily and we assume that the value of the t_c is not reached. One may consider the approach as an intermediate “heuristic” approach that may be used in the future to develop an autonomous (and not time-dependent) model for diffusion-controlled kinetics.

2.1.2. Dissociation rate coefficient

The diffusion of the dissociated particle (receptor or analyte) from the solid surface (e.g. analyte–receptor complex coated surface) into the solution may be given as a first approximation by:

$$(\text{analyte.receptor}) \sim -t^{(3-D_{f,\text{diss}})/2} (t > t_{\text{diss}}) \quad (1b)$$

Here $D_{f,\text{diss}}$ is the fractal dimension of the surface for the desorption step. t_{diss} represents the start of the dissociation step. This corresponds to the

highest concentration of the analyte–receptor on the surface. Henceforth, its concentration only decreases. $D_{f,bind}$ may or may not be equal to $D_{f,diss}$.

The equilibrium dissociation constant (or affinity), $K_D (= k_{diss}/k_{bind})$ can be calculated using the above models. The ratio besides providing physical insights into the analyte–receptor system is of practical importance since it may be used to help determine (and possibly enhance) the regenerability, reusability, stability, and other biosensor performance parameters.

2.2. Dual-fractal analysis

2.2.1. Binding rate coefficient

The single-fractal analysis we have just presented is extended to include two fractal dimensions. At present, the time ($t = t_1$) at which the first fractal dimension “changes” to the second fractal dimension is arbitrary and empirical. For the most part it is dictated by the data analyzed and the experience gained by handling a single-fractal analysis. A smoother curve is obtained in the “transition” region, if care is taken to select the correct number of points for the two regions. In this case, the analyte–receptor complex is given by:

$$\begin{aligned} & \text{(analyte.receptor)} \\ & \sim \begin{cases} t^{(3-D_{f1,bind})/2} = t^{p1} (t < t_1) \\ t^{(3-D_{f2,bind})/2} = t^{p2} (t_1 < t < t_2 = t_c) \\ t^{1/2} (t > t_c) \end{cases} \quad (1c) \end{aligned}$$

2.2.2. Dissociation rate coefficient

Once again similar to the binding rate coefficient(s), we propose that a similar mechanism is involved (except in reverse) for the dissociation step. In this case, the dissociation takes place from a fractal surface. The diffusion of the dissociated particle (receptor or analyte) from the solid surface (e.g. analyte–receptor complex coated surface) into the solution may be given as a first approximation by:

(analyte.receptor)

$$\sim \begin{cases} -t^{(3-D_{f1,diss})/2} (t_{diss} < t < t_{d1}) \\ -t^{(3-D_{f2,diss})/2} (t_{d1} < t < t_{d2}) \end{cases} \quad (1d)$$

Note that different combinations of the binding and dissociation steps are possible as far as the fractal analysis is concerned. Each of these steps or phases can be represented by either a single- or a dual-fractal analysis.

3. Results

At the outset it is appropriate to indicate that a fractal analysis will be applied to the data obtained for analyte–receptor binding and dissociation data for different biosensor systems. The analyte–receptor binding as well as the dissociation reaction is a complex reaction, and the fractal analysis via the fractal dimension (either $D_{f,bind}$ or $D_{f,diss}$) and the rate coefficient for binding (k_{bind}) or dissociation (k_{diss}) provide a useful lumped parameter(s) analysis of the diffusion-limited situation.

Also, we do not present any independent proof or physical evidence for the existence of fractals in the analysis of these analyte–receptor binding/dissociation systems except by indicating that it is a convenient means to make more quantitative the degree of heterogeneity that exists on the surface. Thus, in all fairness, this is one possible way by which to analyze this analyte–receptor binding/dissociation data. One might justifiably argue that appropriate modeling may be achieved by using a Langmuirian or other approach. In fact the analysis software generally supplied with the biosensors, models the kinetic interactions using 1:1 Langmuir binding, Langmuir Binding with mass transfer, steady-state affinity models, etc., but does not present any models that take into account the surface heterogeneity or roughness generally present on these biosensor surfaces.

Lee and Lee (1995) indicate that the fractal approach has been applied to surface science, for example, adsorption and reaction processes. These authors emphasize that the fractal approach provides a convenient means to represent the different structures and morphology at the reaction surface. They also emphasize using the fractal

approach to develop optimal structures and as a predictive approach.

Our analysis, at present, does not include the nonselective adsorption of an analyte. We do recognize that, in some cases, this may be a significant component of the adsorbed material and that this rate of association, which is of a temporal nature, would depend on surface availability. If we were to accommodate the nonselective adsorption into the model, there would be an increase in the degree of heterogeneity on the surface, since by its very nature nonspecific adsorption is more heterogeneous than specific adsorption. This would lead to higher fractal dimension values since the fractal dimension is a direct measure of the degree of heterogeneity that exists on the surface. For a first-order reaction, as expected, an increase in the heterogeneity on the surface due to non-specific binding would lead to lower values of the (specific) binding rate coefficient. The deletion of this non-specific binding in the analysis leads to (artificially) higher values of the binding rate coefficient for first-order reactions.

Our reactions are, in general, higher than first-order. Sadana and Chen (1996) have shown that for reaction orders higher than one a certain amount of heterogeneity is beneficial for the binding rate coefficient. There is apparently an optimum range, which is due to steric factors. Thus, depending on whether one is inside or outside this optimum range, the deletion of non-specific binding in the analysis would lead to either an increase or a decrease in the binding rate coefficient. In other words, if one is in the optimum range, for a particular reaction order, then the presence of non-specific binding would lead to higher values of the (specific) binding rate coefficient. In this case, the deletion of the non-specific binding leads to lower than real-life values of the binding rate coefficient.

Liu et al. (2000) have utilized a molecular beacon DNA sensor to analyze the binding of 1-base mismatch oligonucleotides in solution and binding of complementary oligonucleotides in solution to biotinylated single stranded (ss) DNA immobilized on the sensor chip surface. The advantage of their technique is that no dye-labeled

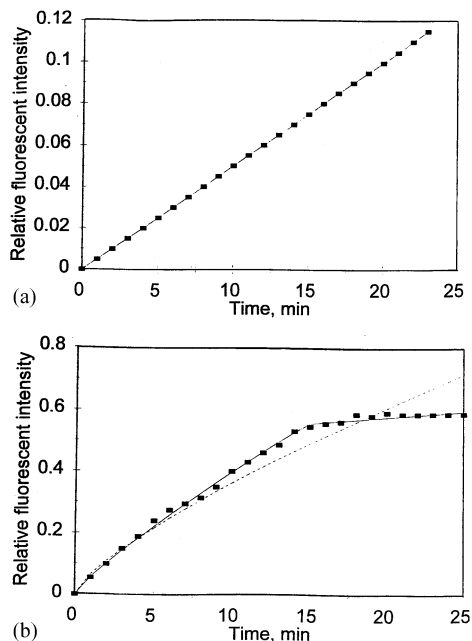


Fig. 1. Binding of oligonucleotide in solution to biotinylated ssDNA molecular beacon immobilized on a SPR biosensor surface (Liu et al., 2000): (a) 1-base mismatch oligonucleotide (■ Liu data, — single fractal fit), (b) 30 nM complementary oligonucleotide (■ Liu data, ---- single fractal fit, — dual fractal fit).

target molecule or an intercalation agent is required. These authors indicate that hairpin-shaped oligonucleotides that report the presence of specific nucleic acids are utilized as molecular beacons. Fig. 1a shows the curves obtained using Eq. (1a) for the binding of 30 nM 1-base mismatch oligonucleotides in solution to a biotinylated ssDNA (molecular beacon) immobilized on an ultra small optical fiber probe. As seen in Fig. 1, single-fractal analysis was adequate to describe the binding kinetics.

Fig. 1b shows the curves obtained for the binding of 30 nM complementary oligonucleotide in solution to a biotinylated ssDNA immobilized on the ultra small optical fiber probe. In this case, a dual-fractal analysis (Eq. (1c)) is adequate to describe the binding kinetics. There is a change in the binding mechanism as one goes from the binding of complementary oligonucleotide (Fig. 1b) to the binding of the 1-base mismatch oligonucleotide (Fig. 1a), since a dual-fractal and a

single-fractal analysis, respectively, are required to describe the binding kinetics. The fit obtained by using a single-fractal analysis for the binding of the complementary oligonucleotide to the ssDNA is depicted by dotted lines in Fig. 1(b). By looking at the fit and the R -squared values obtained it was determined that a single-fractal analysis is not sufficient and that the dual-fractal model needs to be employed. Generally for our analysis we consider R^2 values greater than 0.97 to be satisfactory.

Table 1 shows (a) the values of the binding rate coefficient, k and the fractal dimension, D_f for a single-fractal analysis, and (b) the values of the binding rate coefficients, k_1 and k_2 , and the fractal dimensions for binding, D_{f1} and D_{f2} for a dual-fractal analysis. The values of the binding rate coefficients and the fractal dimensions presented in Table 1 were obtained from a regression analysis using Corel Quattro Pro 8.0 (Corel Corporation, 1997) to model the experimental data using Eq. (1a), wherein $[\text{analyte.receptor}] = kt^p$ for the binding step. The binding rate coefficient values presented in Table 1 are within 95% confidence limits. For example, for the binding of 30 nM complementary oligonucleotide in solution to a biotinylated ssDNA molecular beacon immobilized on the optical fiber probe k_1 is equal 0.058 ± 0.002 . The 95% confidence limits indicates that 95% of the k_1 values will lie between 0.056 and 0.060. This indicates that the values presented are precise and significant. The curves presented in the figures are theoretical curves.

It is surprising to note that the binding of a 1-base mismatch oligonucleotide in solution to the molecular beacon biosensor requires only a single-fractal (simple) mechanism whereas the binding of a complementary oligonucleotide in solution to the

molecular beacon biosensor requires a dual-fractal (complex) mechanism. At the outset, it would appear that this should be the other way around. However, no explanation is offered at present for this, except for maybe the fact that there is, as expected, a stronger binding of the complementary strand and since DNA hybridization reactions are very specific, even a single pair mismatch would decrease the binding and the amount of double stranded DNA formed. This fact is further strengthened by the fact that the k , k_1 , and k_2 values for the binding of the complementary strand are much higher than the k values obtained when there is even a single base mismatch. We do not present any other independent proof confirming the above, except stating that more experiments need to be performed with different oligonucleotide modules at different concentrations having possibly more than a single base pair mismatch.

Wink et al. (1999) have analyzed the binding of plasmid DNA in solution to a cationic polymer immobilized on a SPR biosensor. Fig. 2a shows the binding of 2 $\mu\text{g/ml}$ plasmid DNA in solution to a non-thiolated poly(L-lysine) polymer layer immobilized on a SPR biosensor surface. A dual-fractal analysis is required to adequately describe the binding kinetics. The values of (a) the binding rate coefficient, k , and the fractal dimension, D_f , for a single-fractal analysis, and (b) the binding rate coefficients, k_1 and k_2 , and the fractal dimensions, D_{f1} and D_{f2} , for a dual-fractal analysis are given in Table 2. It is of interest to note that for the dual-fractal analysis as the fractal dimension for binding increases from D_{f1} to D_{f2} , the binding rate coefficient increases from k_1 to k_2 . A 30.8% increase in the fractal dimension from a value of

Table 1

Influence of non-complementary oligonucleotide and 1-base mismatch oligonucleotide on the binding rate coefficients and fractal dimensions for a hybridization reaction using an immobilized molecular beacon optical fiber biosensor (Liu et al., 2000)

Analyte in solution/receptor on surface	k	D_f	k_1	k_2	D_{f1}	D_{f2}
30 nM 1-base mismatch oligonucleotide/biotinylated ssDNA molecular beacon	0.005	2.00	na	na	na	na
30 nM complementary oligonucleotide/biotinylated ssDNA molecular beacon	0.066 ± 0.01	1.52 ± 0.05	0.058 ± 0.002	0.389 ± 0.006	1.32 ± 0.03	2.74 ± 0.06

na: not applicable.

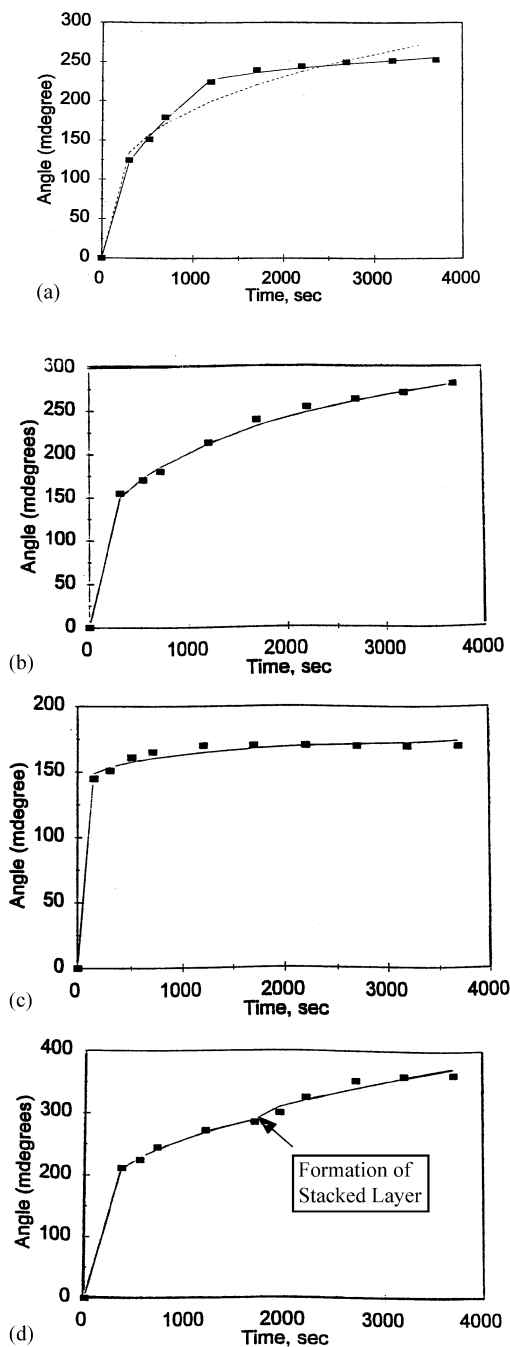


Fig. 2. Binding of plasmid DNA (in $\mu\text{g/ml}$) in solution to non-thiolated poly(L-lysine) immobilized on a SPR biosensor surface (Wink et al., 1999): (a) 2 (\blacksquare Wink data, ---- single fractal fit, — dual fractal fit), (b) 4 (c) 8 (d) 10 (\blacksquare Wink data, — single fractal fit).

D_{f1} equal to 2.14 to D_{f2} equal to 2.80 leads to an increase in the binding rate coefficient by a factor of 10.47 from a value k_1 equal to 10.6 to a value of k_2 equal to 111. In other words, an increase in the degree of heterogeneity on the surface as the reaction proceeds leads to an increase in the binding rate coefficient.

Fig. 2b shows the binding of 4 $\mu\text{g/ml}$ of plasmid DNA in solution to a non-thiolated poly(L-lysine) polymer layer immobilized on a SPR biosensor surface. A single-fractal analysis is sufficient to describe the binding kinetics adequately. The values of the binding rate coefficients and the fractal dimensions are given in Table 2. It is of interest to note that an increase in the plasmid DNA (analyte) concentration in solution from 2 to 4 $\mu\text{g/ml}$ leads to a ‘simpler’ binding mechanism. At the lower (2 $\mu\text{g/ml}$) analyte concentration a dual-fractal analysis is required, whereas at the higher (4 $\mu\text{g/ml}$) analyte concentration a single-fractal analysis is required to describe the binding kinetics adequately.

We do not offer any other explanations for the change from dual to a single-fractal mechanism at the higher concentrations. It is possible that the experiment is not conducted at a high enough time resolution to see the dual-fractal mechanism at the 4 $\mu\text{g/ml}$ concentration and higher. Perhaps, the “second” fractal behavior is revealed only at these late times. In essence, the increased reactant densities in the later experiments hide the early time behavior except in the 2 $\mu\text{g/ml}$ case.

Fig. 2c shows the binding of 8 $\mu\text{g/ml}$ of plasmid DNA in solution to a non-thiolated poly(L-lysine) polymer layer immobilized on a SPR biosensor surface. Once again, a single-fractal analysis is sufficient to describe the binding kinetics adequately. The values of the binding rate coefficients and the fractal dimensions are given in Table 2. Fig. 2d shows the binding of 10 $\mu\text{g/ml}$ of plasmid DNA in solution to a non-thiolated poly(L-lysine) polymer layer immobilized on a SPR biosensor surface. Here too, a single-fractal analysis is sufficient to describe the binding kinetics adequately. The values of the binding rate coefficients and the fractal dimensions are given in Table 2. In this case, however, due to the high concentration of analyte in solution, there is a formation of a

Table 2

Influence of plasmid DNA concentration on binding rate coefficients and fractal dimensions for its binding to (a) nonthiolated poly(L-lysine) and (b) poly[2-(dimethylamino) ethylmethacrylate] (p-DMAEMA) immobilized on a SPR biosensor (Wink et al., 1999)

Analyte in solution/receptor on surface	k	D_f	k_1	k_2	D_{f1}	D_{f2}
(a) 2 $\mu\text{g/ml}$ plasmid DNA/nonthiolated poly(L-lysine)	26.5 ± 2.10	2.43 ± 0.06	10.6 ± 0.28	111 ± 1.49	2.14 ± 0.05	2.80 ± 0.03
4 $\mu\text{g/ml}$ plasmid DNA/nonthiolated poly(L-lysine)	36.5 ± 0.81	2.50 ± 0.02	na	na	na	na
8 $\mu\text{g/ml}$ plasmid DNA/nonthiolated poly(L-lysine)	116.1 ± 2.73	2.90 ± 0.01	na	na	na	na
10 $\mu\text{g/ml}$ plasmid DNA/nonthiolated poly(L-lysine)	65.2 ± 0.92	2.59 ± 0.02	$k_{\text{stack}} = 34.9$	na	$D_{f,\text{stack}} = 2.60$	na
(b) 2 $\mu\text{g/ml}$ plasmid DNA/5%-thiolated p-DMAEMA	3.40 ± 0.26	2.38 ± 0.06	na	na	na	na
6 $\mu\text{g/ml}$ plasmid DNA/5%-thiolated p-DMAEMA	10.4 ± 0.34	2.43 ± 0.03	na	na	na	na
10 $\mu\text{g/ml}$ plasmid DNA/5%-thiolated p-DMAEMA	44.7 ± 0.80	2.61 ± 0.01	na	na	na	na

na: not applicable.

'stacked layer.' The authors (Wink et al., 1999) clearly indicate the presence of a stacked layer. During the initial period, (at time, t close to zero), the binding is adequately described by a single-fractal analysis. During the stacked layer, the binding rate coefficient, k is lower in value (equal to 34.9) than in the initial phase (equal to 65.2). Also, the fractal dimension during the stacked phase equal to 2.60 is however, almost the same as the fractal dimension during the initial phase (equal to 2.59).

In other words, in this case, though the fractal dimension remains nearly the same during the two phases (initial and stacked) there is a 46.47% decrease in the binding rate coefficient as one goes from the initial phase to the stacked phase of binding. This is of interest since it provides a possible means, or exhibits the potential of manipulating (in this case, decreasing) the binding rate coefficient. Only a single example is provided, and more data need to be analyzed using the stacked layer to see if one may manipulate binding rate coefficients in desired directions utilizing one (or even two or more stacked) layers. Note that since the binding of the initial layer (close to time, t equal to zero) and that of the stacked layer may be described by a single-fractal analysis, this indicates that there is, at least, some similarity in the binding mechanism.

Fig. 3a shows the binding of 2 $\mu\text{g/ml}$ plasmid DNA in solution to 5% thiolated pDMAEMA immobilized on a SPR biosensor surface (Wink et al., 1999). A single-fractal analysis is adequate to describe the binding kinetics. The values of the

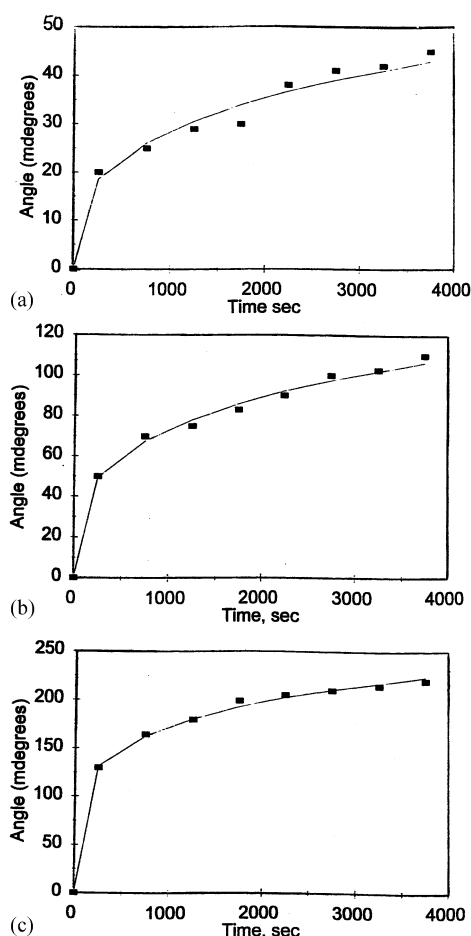


Fig. 3. Binding of plasmid DNA (in $\mu\text{g/ml}$) in solution to 5% thiolated poly(L-lysine) immobilized on a SPR biosensor surface (Wink et al., 1999): (a) 2 (b) 6 (c) 10 (■ Wink data, — single fractal fit).

binding rate coefficient, k , and the fractal dimension, D_f , are given in Table 2 b. Fig. 3b and c show the binding of 6 and 10 $\mu\text{g/ml}$ DNA in solution to 5% thiolated pDMAEMA immobilized on a SPR biosensor surface. Once again, a single-fractal analysis is adequate to describe the binding kinetics. The values of the binding rate coefficient and the fractal dimensions are given in Table 2.

We have developed predictive expressions trying to link the binding rate coefficient, k , and the fractal dimension, D_f , to the plasmid DNA concentration in solution. The prefactor analysis for fractal aggregates, provided by Sorenson and Roberts (1997) was used to generate these predictive expressions. Also, we have developed an expression that relates the binding rate coefficient to the degree of heterogeneity or fractal dimension existing on the surface for the binding of 2, 6 and 10 $\mu\text{g/ml}$ DNA in solution to 5% thiolated pDMAEMA immobilized on a chip (Wink et al., 1999). Fig. 4a and Table 2 show that as the plasmid concentration in solution increases from 2 to 10 $\mu\text{g/ml}$ the binding rate coefficient, k , increases.

In the 2–10 $\mu\text{g/ml}$ plasmid concentration range analyzed, the binding rate coefficient, k is given by:

$$k = (1.050 \pm 0.702) [\text{plasmid DNA}]^{1.51 \pm 0.44} \quad (3a)$$

The binding rate coefficient is mildly sensitive to the plasmid DNA concentration in solution in the range analyzed, and exhibits close to a one and a half-order dependence. More data points are required to more firmly establish this relation. Nevertheless, Eq. (3a) is of value since it provides a quantitative indication of how the binding rate coefficient, k , changes with plasmid concentration in solution.

It is not surprising to obtain a power-law equation, Eq. (3a), linking the binding rate coefficient and the fractal dimension given the fractal nature of the biosensor surface. It is not our intention to prove fractality using the above equation. In fact, it is not necessary for a power-law equation to be applicable every time fractal kinetics are employed. The purpose of Eq. (3a) is to study the relationship (sensitivity) of the bind-

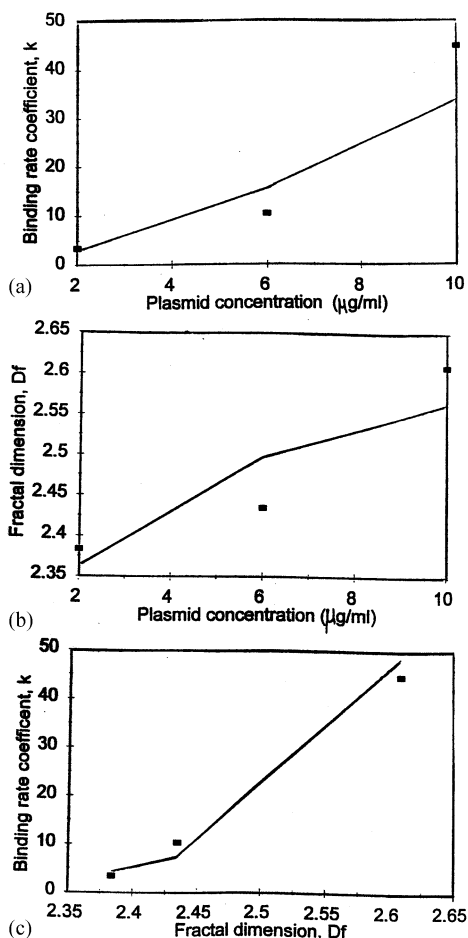


Fig. 4. Predictive expressions linking the binding rate coefficient, k and fractal dimension, D_f , to the plasmid DNA concentration and also the binding rate coefficient, k and the fractal dimension D_f (data from Table 2b and Fig. 3). (a) Increase in the binding rate coefficient, k with an increase in the plasmid DNA concentration. (b) Increase in the fractal dimension, D_f with an increase in the plasmid DNA concentration. (c) Increase in the binding rate coefficient, k with an increase in the fractal dimension, D_f .

ing rate coefficient to the fractal dimension or degree of heterogeneity existing on the surface.

Fig. 4b and Table 2 show that as the plasmid DNA concentration in solution increases from 2 to 10 $\mu\text{g/ml}$, the fractal dimension, D_f increases. In the 2–10 $\mu\text{g/ml}$ plasmid DNA concentration range analyzed, the fractal dimension, D_f is given by:

$$D_f = (2.28 \pm 0.08) [\text{plasmid DNA}]^{0.05 \pm 0.03} \quad (3b)$$

The fractal dimension, D_f , exhibits only a very low dependence on the plasmid DNA concentration in solution. The fractal dimension increases very slowly with an increase in the plasmid DNA concentration in solution.

Fig. 4c and Table 2 show that the binding rate coefficient, k , increases as the fractal dimension, D_f , increases. For the data presented in Table 2, the binding rate coefficient, k , is given by:

$$k = (3.57 \times 10^{-10} \pm 1.78 \times 10^{-10}) D_f^{26.73 \pm 6.05} \quad (3c)$$

For the three data points presented in Fig. 4c the fit is quite reasonable. More data points would more firmly establish this relation. The binding rate coefficient, k , is extremely sensitive to the degree of heterogeneity that exists on the surface as noted by the very high value of the exponent. Note also the very low value of the coefficient (equal to 3.57×10^{-10}).

Wink et al. (1999) have also analyzed the reversibility of plasmid DNA/pDMAEMA complex formation. At a pH of 7.4 the plasmid DNA in solution was bound to the 5%-thiolated pDMAEMA immobilized on the SPR biosensor surface. As the pH was changed to 8.8 the plasmid DNA/pDMAEMA complex on the SPR biosensor surface dissociated. They showed such data for two cycles.

Fig. 5 shows that a dual-fractal analysis is required to describe the binding kinetics adequately. However, a single-fractal analysis is required to describe the dissociation kinetics. The values of the binding rate coefficient, k , and the

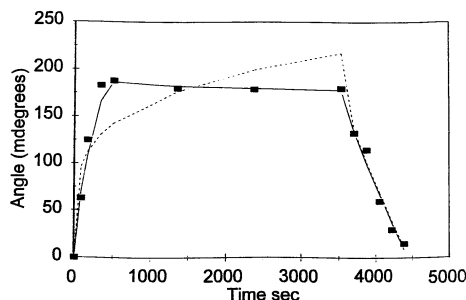


Fig. 5. Reversibility of plasmid DNA/poly[2-(dimethyl)ethylmethacrylate] (p-DMAEMA) complex binding on a SPR biosensor surface (Wink et al., 1999). (■ Wink data, ---- single fractal fit, — dual fractal fit).

fractal dimension, D_f , for a single-fractal analysis, the binding rate coefficients, k_1 and k_2 , and the fractal dimensions, D_{f1} and D_{f2} , for a dual-fractal analysis and the dissociation rate coefficient, k_{diss} (or k_d) and the fractal dimension for dissociation, $D_{f,\text{diss}}$ (or D_{fd}), are given in Table 3. It is of interest to note that as the fractal dimension for binding increases by about 70% from a value of 1.76 to a maximum value of 3.0, the binding rate coefficient, k , increases by a factor of 348.9.

It is of interest to compare the binding of plasmid DNA in solution to non-thiolated and 5% thiolated pDMAEMA immobilized on the sensor surface. From Table 2 one notes that comparisons can be made for the 2 and 10 $\mu\text{g/ml}$ plasmid DNA concentration in solution. The binding of 2 $\mu\text{g/ml}$ plasmid DNA in solution to the non-thiolated pDMAEMA immobilized on the SPR biosensor surface requires a dual-fractal analysis to adequately describe the binding kinetics. The binding of 2 $\mu\text{g/ml}$ plasmid DNA in solution to 5% thiolated pDMAEMA immobilized on the SPR biosensor surface requires a single-fractal analysis. This indicates that there is a change in the binding mechanism as one goes from the non-thiolated pDMAEMA immobilized in the SPR surface to the 5% thiolated pDMAEMA immobilized on the SPR surface. Since a dual-fractal analysis is required for the non-thiolated case, this indicates that in this case a complex binding mechanism is involved.

It is also of interest to compare the binding of 10 $\mu\text{g/ml}$ plasmid DNA in solution to a non-thiolated as well as the thiolated case. For both of these cases, a single-fractal analysis is sufficient to adequately describe the binding kinetics when time, t , is close to zero. Note that although the values of the fractal dimension, D_f , are close to each other (2.59 for non-thiolated case and 2.61 for the thiolated case) the values of the binding rate coefficient are quite different from each other. The binding rate coefficient for the non-thiolated surface is higher than the binding to the thiolated surface by 44.8%. Note, however, that for the non-thiolated case there is a stacked layer of binding too as indicated earlier.

As mentioned earlier, Wink et al. (1999) also studied the dissociation of the Plasmid DNA/p-

Table 3

Influence of reversibility of plasmid DNA/poly[2-dimethyl]ethylmethacrylate] (p-DMAEMA) complex formation on binding, dissociation, and fractal dimensions using a SPR biosensor (Wink et al., 1999)

Analyte in solution/receptor on surface	k	D_f	k_1	k_2	k_d	D_{f1}	D_{f2}	D_{fd}
Plasmid DNA/5%p-DMAEMA	36.9 ± 12.6	2.57 ± 0.17	4.46 ± 0.83	217 ± 2.9	0.574 ± 0.08	1.76 ± 0.25	3.0	1.31 ± 0.21

DMAEMA complex from the biosensor surface at pH 8.8. As indicated before, a single-fractal analysis using Eq. (1b) was sufficient to describe the dissociation kinetics. The fractal dimension for dissociation, D_{fd} equal to 1.31 is smaller than both the fractal dimensions for binding (D_{f1} equal to 1.76 and D_{f2} equal to 3.0). Finally, it is of interest to present values of the affinity, K_D , K_{D1} ($=k_{diss}/k_1$) = 0.129, and K_{D2} ($=k_{diss}/k_2$) = 0.0026.

4. Conclusion

A fractal analysis of the binding of antigen (or antibody) in solution to antibody (or antigen) immobilized on the biosensor surface provides a quantitative indication of the state of disorder (fractal dimension, $D_{f,bind}$) and the binding rate coefficient, k_{bind} , on the surface. In addition, fractal dimensions for the dissociation step, $D_{f,diss}$, and dissociation rate coefficients, k_{diss} , are also presented. This provides a more complete picture of the analyte–receptor reactions occurring on the surface in contrast to an analysis of the binding step alone, as done previously (Sadana, 1999). Besides, one may also use the numerical values for the rate coefficients for binding and the dissociation steps to classify the analyte–receptor biosensor system.

The fractal dimension value provides a quantitative measure of the degree of heterogeneity that exists on the surface for the analyte–receptor systems. The degree of heterogeneity for the binding and the dissociation phases is, in general, different for the same reaction. This indicates that the same surface exhibits two degrees of heterogeneity for the binding and the dissociation reaction. Both types of examples are given wherein either a single- or a dual-fractal analysis is required to describe the binding kinetics. The dual-fractal

analysis was used only when the single-fractal analysis did not provide an adequate fit. The dissociation step was described adequately by a single-fractal analysis for the single example presented.

In accord with the prefactor analysis for fractal aggregates (Sorenson and Roberts, 1997), a quantitative (predictive) expression is developed for the binding rate coefficient as a function of the fractal dimension for binding. The parameter, K_D ($=k_{diss}/k_{bind}$) value presented is of interest since it provides an indication of the stability, reusability, and regenerability of the biosensor. Also, depending on one's final goal, a higher or a lower K_D value may be beneficial for a particular analyte–receptor system. During the binding of 8 $\mu\text{g}/\text{ml}$ of plasmid DNA in solution to a non-thiolated poly(L-lysine) polymer immobilized on a SPR biosensor surface there was the distinct formation of a stacked layer (Wink et al., 1999). It is of interest to note that the fractal dimension remains almost the same during the initial phase at time, t , close to zero ($D_f = 2.59$), and during the stacked phase ($D_f = 2.60$). However, the binding rate coefficient (k equal to 34.9) is 46.6% lower during the stacked phase as compared to the initial phase ($k = 65.2$). If indeed this is true, then perhaps this may exhibit the potential to decrease (or manipulate) the binding rate coefficient in a desired direction (in this case decreasing). Much more data need to be analyzed to show if indeed this is true.

The fractal dimension for the binding or the dissociation phase, $D_{f,bind}$ or $D_{f,diss}$, respectively, is not a typical independent variable, such as analyte concentration, that may be manipulated directly. It is estimated from Eqs. (1a) and (1c), and one may consider it as a derived variable. The predictive relationship developed for the binding rate coefficient as a function of the fractal dimension is of considerable value because it directly links the

binding rate coefficient to the degree of heterogeneity that exists on the surface, and suggests a means by which the binding rate coefficient may be manipulated by changing the degree of heterogeneity that exists on the surface. Note that a change in the degree of heterogeneity on the surface would, in general, lead to changes in both the binding and perhaps in the dissociation rate coefficient, too. Thus, this may require a little thought and manipulation.

Generally it is seen that an increase in the fractal dimension of the surface or the degree of heterogeneity leads to an increase in the binding rate coefficient. One possible explanation of the observed increase could be due to the fact that the fractal surface (roughness) leads to turbulence, which enhances mixing, decreases diffusional limitations, and leads to an increase in the binding rate coefficient (Martin et al., 1991). Granted, for this to occur, the characteristic length of this turbulent boundary layer may have to extend a few monolayers above the sensor surface to affect the bulk diffusion to and from the surface. Considering the extremely laminar flow regimes in most biosensors this may not be possible. However, due to the fractal nature of the surface that involves, for example, grooves and ridges, the surface morphology may contribute substantially towards the presence of eddy diffusion. This eddy diffusion enhances mixing and helps extend the characteristic length of the boundary layer to affect the bulk diffusion to and from the surface.

The characterization of the surface by a fractal dimension provides extra flexibility and suggests an avenue whereby the nature of the surface may be modulated in desired directions, and thereby simultaneously affecting or changing the dissociation and binding rate coefficients in required directions. This predictive approach is of considerable value in the design of biosensor experiments. More such studies are required to determine whether the binding and the dissociation rate coefficient are sensitive to their respective fractal dimensions or the degree of heterogeneity that exists on the biosensor surface. If this is correct, then experimentalists may find it worth their effort to pay a little more attention to the nature of the surface, and how it may be manipulated to control

the relevant parameters and biosensor performance in desired directions. Also, in a more general sense, the treatment should also be applicable to non-biosensor applications wherein further physical insights could be obtained.

Acknowledgements

Support from a Congressional Initiative awarded to the University of Mississippi is greatly appreciated. The initiative is entitled "A Virtual Center for Disease Prevention in Humans and Ecosystems" [CDC RO6/CCR419466-02].

References

- Corel Quattro Pro 8.0, 1997. Corel Corporation Limited, Ottawa, Canada.
- Havlin, S., 1989. Molecular diffusion and reactions. In: Avnir, D. (Ed.), *The Fractal Approach to Heterogeneous Chemistry: Surfaces, Colloids, Polymers*. Wiley, New York, pp. 251–269.
- Jonsson, U., Fagerstam, L., Ivarsson, B., Johnsson, B., Karlsson, R., Lundh, K., Lofas, S., Kakabakos, S., Christopoulos, T., Diamindis, E., 1992. *Clin. Chem.* 38, 338–342.
- Kopelman, R., 1988. Fractal reaction kinetics. *Science* 241, 1620–1626.
- Lee, C.K., Lee, S.L., 1995. Multi-fractal scaling analysis of reactions over fractal surfaces. *Surface Sci.* 325, 294–310.
- Liu, X., Farmerie, W., Schuster, S., Tan, W., 2000. Molecular beacons for DNA biosensors with micrometer to submicrometer dimensions. *Anal. Biochem.* 283, 175–181.
- Markel, V.A., Muratov, L.S., Stockman, M.I., George, T.F., 1991. *Phys. Rev. B* 43 (10), 8183–8195.
- Martin, S.J., Granstaff, V.E., Frye, G.C., 1991. Effect of surface roughness on the response of thickness-shear mode resonators in liquids. *Anal. Chem.* 65, 2910–2922.
- Myszka, D.G., Morton, T.A., Doyle, M.L., Chaiken, I.M., 1997. Kinetic analysis of a protein antigen–antibody interaction limited by mass transfer on an optical biosensor. *Biophys. Chem.* 64, 127–137.
- Pajkossy, T., Nyikos, L., 1989. Diffusion to fractal surfaces. II. Verification of theory. *Electrochim. Acta* 34 (2), 71–179.
- Pfeifer, P., Obert, M., 1989. Fractals: basic concepts and terminology. In: Avnir, D. (Ed.), *The Fractal Approach to Heterogeneous Chemistry: Surfaces, Colloids, Polymers*. Wiley, New York, pp. 11–43.
- Ramakrishnan, A., Sadana, A., 2001. A fractal analysis for cellular analyte–receptor binding kinetics; biosensor applications. *Automedica*, 1–28.

- Sadana, A., 1999. A single- and a dual-fractal analysis of antigen–antibody binding kinetics for different biosensor applications. *Biosens. Bioelectron.* 14, 515–531.
- Sadana, A., 2001. A kinetic study of analyte–receptor binding and dissociation, and dissociation alone for biosensor applications. A fractal analysis. *Anal. Biochem.* 291 (1), 34–47.
- Sadana, A., Chen, Z., 1996. A fractal analysis of the influence of non-specific binding on antigen–antibody binding kinetics for biosensor applications. *Biosens. Bioelectron.* 11 (8), 769–782.
- Sorenson, C.M., Roberts, G.C., 1997. The prefactor of fractal aggregates. *J. Colloid Interface Sci.* 186, 447–452.
- Williams, C., Addona, T.A., 2000. The integration of SPR biosensors with mass spectrometry: possible applications for proteome analysis. *Trends in Biotechnol.* 18, 45–48.
- Wink, T., de Beer, J., Hennick, W.E., Bult, A., van Bennekom, W.P., 1999. Interaction between plasmid DNA and cationic polymers studied by surface plasmon resonance spectroscopy. *Anal. Chem.* 71, 801–805.